Thermochimica Acta 503–504 (2010) 121–131

Contents lists available at ScienceDirect

Thermochimica Acta

journal homepage: www.elsevier.com/locate/tca

Enthalpy and entropy changes on structural relaxation of $Mg_{65}Cu_{25}Tb_{10}$ glass

Daisman P.B. Aji, G.P. Johari*

Department of Materials Science and Engineering, McMaster University, 1280, Main Street West, Hamilton, Ontario L8S 4L7, Canada

ARTICLE INFO

Article history:
Received 22 December 2009
Received in revised form 10 March 2010
Accepted 25 March 2010
Available online 31 March 2010

Keywords:
Metal alloy glass
Structural relaxation
Fictive temperature
Enthalpy and entropy

ABSTRACT

Changes in the enthalpy and entropy on structural relaxation of $Mg_{65}Cu_{25}Tb_{10}$ glass have been studied after keeping its samples for varying periods of time t_a at several temperatures T_as, and after keeping for fixed t_a at various T_as. At a fixed T_a, the decrease in the enthalpy and entropy occurred with time according to a non-exponential kinetics. When the sample was kept for the same t_a, but at different T_as, the decrease in the enthalpy and entropy showed a peak at a temperature when the sample reached an equilibrium state for that t_a. The fictive temperature estimated from the entropy change was the same as that estimated from the enthalpy change, thus suggesting that irreversibility of the thermodynamic path in the glass-transition range does not have a significant effect on determining the entropy. The rate of heat release from the DSC heating scan was analyzed in terms of the model for non-exponential, non-linear enthalpy relaxation. A single set of parameters that fitted the data for un-annealed glass did not fit the data for the highly annealed glass. This is expected in view of the approximations made in the model and the contribution from the JG relaxation. It is suggested that a model-independent method for studying enthalpy relaxation would be more appropriate. A glass stored at ambient conditions showed an endothermic peak that is attributed partly to the unfreezing of the JG relaxation and partly to those of the faster modes in the distribution of the α-relaxation times.

1. Introduction

A characteristic feature of glass is that its properties at a fixed temperature change with time toward those of the equilibrium state [1–11], a phenomenon known as structural relaxation. It occurs also when a glass is slowly heated toward its glass softening or T_g range [8,11]. In this process, (i) the net enthalpy H and entropy S decrease, (ii) the size of the co-operatively rearranging region would increase according to the configurational entropy theory [12], and (iii) the free volume fraction of the volume would decrease according to the free volume theory [13]. There are also changes in the dielectric, mechanical, optical and related properties of a glass with time, t, and temperature T, and these are modeled by using formalisms [14] that express the change in terms of a macroscopic quantity fictive temperature T_f [15], defined as the temperature at which a liquid's structures kinetically freezes on cooling. (It is also defined as the temperature at which a glass would be in internal equilibrium, or a glass and its melt would have the same physical property.) T_f of a solid is high when it is formed by vapor deposition, hyperquenching a liquid, mechanical deformation and pressure collapse of crystals, chemical reaction and lyophilization, and T_f is low when a glass is formed by slowly cooling a melt. T_f decreases continuously as a glass structure relaxes. Different properties yield different T_f values, and T_f determined by one technique is unique for a given thermal history of the sample and is seen therefore as an indication of thermal history of glass. Properties of a state obtained by rapid heating of a glass to T above T_g also change with t, and in this case H and S increase, and T_f increases with time and T [14].

Metal alloy glasses are formed by cooling the melt more rapidly than for forming other glasses and their T_f is relatively high. During storage or use as a device, their structure continuously relaxes and they may crystallize over a long time period, to the detriment of their useful properties. More recently, several ternary and quaternary compositions of metal alloys have been found to form a glassy state by cooling the melt at a relatively slow rate of less than 5 K/min [16–18]. These glasses differ from monocomponent glasses in that they have entropy of mixing which is in addition to the usual configurational entropy. A brief review of their thermodynamics has been given in the Introduction of a paper on the calorimetric study of the "memory effect" [19].

Like organic polymers and inorganic glasses, metal–alloy glasses are seen to have a discipline of their own. But unlike other glasses, (atomic) entities that form their structure have no rotational degrees of freedom. Therefore all diffusive motions in metallic glasses and melts are translational. Their structure also resembles the structure of packed spheres of different sizes representing atoms of different elements, interacting by relatively free electrons,

* Corresponding author. Tel.: +1 905 525 9140; fax: +1 905 528 9295.
E-mail address: joharig@mcmaster.ca (G.P. Johari).

0040-6031/$ – see front matter © 2010 Elsevier B.V. All rights reserved.
doi:10.1016/j.tca.2010.03.021

akin to the model for which computer simulations are performed. It has been occasionally considered that such glasses have both topological and chemical short range order [20,21], but studies of glass relaxation could not confirm its consequences [22,23].

Structural relaxation in metallic glasses has been extensively studied by Chen [24,25], Scott et al. [26–28], Berry and Pritchet [29,30], Egami et al. [31–34], Taub et al. [35,36], Johari et al. [19,22,23,37,38] and Tiwari et al. [39]. Based on the study of structural relaxation in multicomponent metallic glasses, Egami [21,40] and Elliot [41] concluded that there is a distinction between the topological short range order (TSRO) and the chemical short range order (CSRO). They have discussed the change of TSRO and CSRO of metallic glasses due to annealing or ageing. X-ray and electron diffraction measurements have been used to test the validity of this concept but little is known about the atomic diffusion processes occurring either during the isothermal annealing or during heating toward T_g. Van den Buekel and Radelaar [42] proposed that TSRO is a slow process which begins after the completion of the fast CSRO process. Based on their study of structural relaxation in several Pd- and (Fe, Ni)-based metal–metaloid glasses and Zr-(Cu,Fe,Ni) binary and ternary metallic glasses, Inoue et al. [43] and Chen and Inoue [44] concluded that structural relaxation at low temperatures occurs by local and medium range rearrangement of the atoms with weak bonding. At high temperatures it occurs by the long range cooperative regrouping of metal and metalloid atoms.

Studies of several metallic glasses showed [22,23] that structural relaxation can be simulated by the same non-exponential, non-linear relaxation as used for polymeric and inorganic glasses, thus indicating a phenomenological similarity between metal–alloy and other glasses when the distribution of self-diffusion times is considered. This similarity led to the conclusion that structural relaxation of metallic glasses instead involves changes in both TSRO and CSRO. Detailed studies of structural relaxation by thermal cycling metallic glasses in a temperature range below T_g led to the conclusion that those local groups of atoms, whose diffusion is fast enough to allow loss of enthalpy and entropy on their approach to an equilibrium configurational state of low energy on annealing, absorb heat to reach their new equilibrium configuration state of higher energy at a higher temperature but still below T_g on heating at a certain rate. Hence each mode of atomic diffusion in the structure has its own 'mini glass-transition temperature', and its apparent reversible relaxation is a reflection of a broad distribution of times arising from temporal and spatial variations in the atoms' environment [22,23].

Here we report a detailed study of structural relaxation of a typical metal alloy glass of ternary composition, $Mg_{65}Cu_{25}Tb_{10}$, by using accurate differential scanning calorimetry (DSC). We do so by performing measurements of isothermal relaxation at a fixed T for different times t, and a fixed t at different T. We also determine the entropy change on structural relaxation and investigate whether such a change can be reliably made from measurements of the specific heat or calorimetric signal in an irreversible process of structural relaxation. We further examine whether the non-exponential, non-linear structural model for relaxation may be valid for such glasses, and investigate the origin of a large endothermic peak that appears at $T < T_g$ after (inadvertent) ageing of $Mg_{65}Cu_{25}Tb_{10}$ glass at ambient conditions. Earlier calorimetric studies of metallic glasses and of some general features of structural relaxation are briefly reviewed.

2. Experimental methods

Ingots of $Mg_{65}Cu_{25}Tb_{10}$ glass were prepared by the group at Institute of Physics and Center for Condensed Matter Physics, Chinese Academy of Sciences, Beijing, China, which they have also studied by other techniques. Their method of preparation was, (i) arc melting of an accurately weighed mixture of pure elements under a titanium-gettered argon atmosphere and (ii) transferring the melt to a water-cooled copper crucible. To homogenize the melt, the glassy solid was melted two to four times. Plate-like specimens of thickness 1–3 mm, width 5–10 mm, and length of 50–100 mm and rod specimens of diameter 3–5 mm and length of 50–100 mm were produced by suction casting in a copper mold. Its glassy nature has been already characterized by diffraction methods and calorimetry [45–48] and their mechanical properties [47,49,50] have been published.

The calorimeter used for the study was a Pyris Diamond PerkinElmer DSC. The instrument was calibrated with indium and zinc by using their melting points and their enthalpy of melting. Argon was used as both a purge gas for the sample and a carrying gas for the intra-cooler. During the course of measurements on a sample, the baseline, temperature calibration and stability of the equipment was frequently checked. An accurately weighed amount of the sample (nominally 7–15 mg) was contained in an aluminum-pan and crimp-sealed. It was transferred to the instrument at ambient temperature. The DSC output in watts ($J\,s^{-1}$) divided by the sample's mass was found to remain within 0.2%. This showed that the effect of the sample's mass on the measured values was negligible. The heating rate was 20 K/min and it served to enhance the features observed for glass-softening and for structural relaxation over the features observed for the 10 K/min or lower heating rates used generally for studying other glasses. All cooling and heating to reach a predetermined temperature of the sample were done at 100 K/min rate. This minimized the errors arising from structural relaxation that may have occurred during such cooling and heating. DSC scans were obtained for all thermal treatment, i.e., heating, cooling and isothermally holding metal alloy glasses, but only the scans obtained during heating through the glass-softening range are shown here. The enthalpy and entropy changes were calculated accurately by transferring the data to Microcal Origin Software and performing all subtractions and integrations by using its mathematical procedure.

3. Results

A $Mg_{65}Cu_{25}Tb_{10}$ glass sample was first heated at a rate of 20 K/min in the calorimeter from 333 K to 573 K. This led to its crystallization on heating to above 460 K, as indicated by a sharp and deep exotherm in Fig. 1(A), which is only shown partly here. The onset crystallization temperature T_x, was 460.8 K and the ultraviscous melt persisted over the 440–460 K temperature range. (These data will be included in a detailed paper on crystallization.) In addition to the usual glass-transition endotherm, Fig. 1(A) shows an endotherm at lower T that is spread over a 25 K range. This is due to the structural relaxation on first heating of the as-cast sample that had been stored for an unknown period. A new as-cast sample was repeatedly heated at rate of 20 K/min and cooled at rate of 20 K/min three times from 333 K to 443 K. Fig. 1(B) shows the DSC scans obtained. The (dH/dt) measured in the DSC scan was multiplied by the atomic weight of $Mg_{65}Cu_{25}Tb_{10}$ and divided by the mass of the sample and further by the heating rate, q_h. This converted it to (dH/dT) in units of J/mol K.

The scan obtained on first heating shows an endotherm at $T < T_g$ corresponding to the irreversible relaxation in Fig. 1(A). Scan 1 in Fig. 1(B) obtained from another sample from the same as-cast stock shows the same feature. Scan 2 that was obtained on subsequent heating after cooling at 20 K/min rate show no such low-temperature endotherm in Fig. 1(B), nor does scan 3 that was obtained similar to scan 2. Scans 2 and 3 also show reversibility of the sample's state and its properties on heating and cooling several

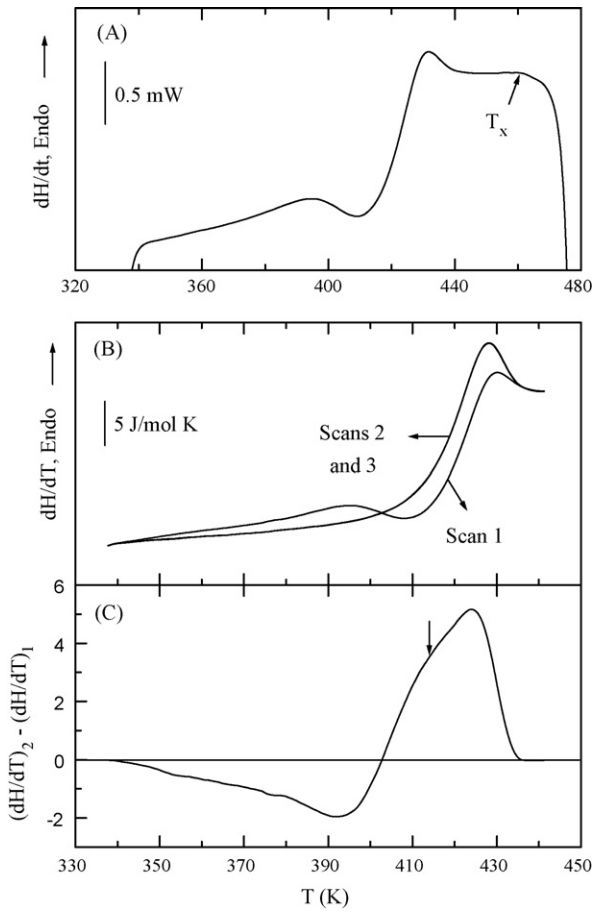

Fig. 1. (A) The DSC scan of an as-cast $Mg_{65}Cu_{25}Tb_{10}$ glass obtained during heating at 20 K/min rate from 333 to 573 K. (B) A second as-cast sample was heated at 20 K/min and DSC scan 1 was obtained. The sample was subsequently cooled at 20 K/min from 443 K to 333 K and then reheated to 443 K at 20 K/min and scan 2 was obtained. Scan 3 was subsequently obtained by the same procedure of cooling and heating. (C) The difference between the heating scans 1 and 2 in (B) is plotted against the temperature. The T_g of 414.2 K, as determined here from the usual line intersection method for scans 2 and 3 in (B) is marked by arrow in (C).

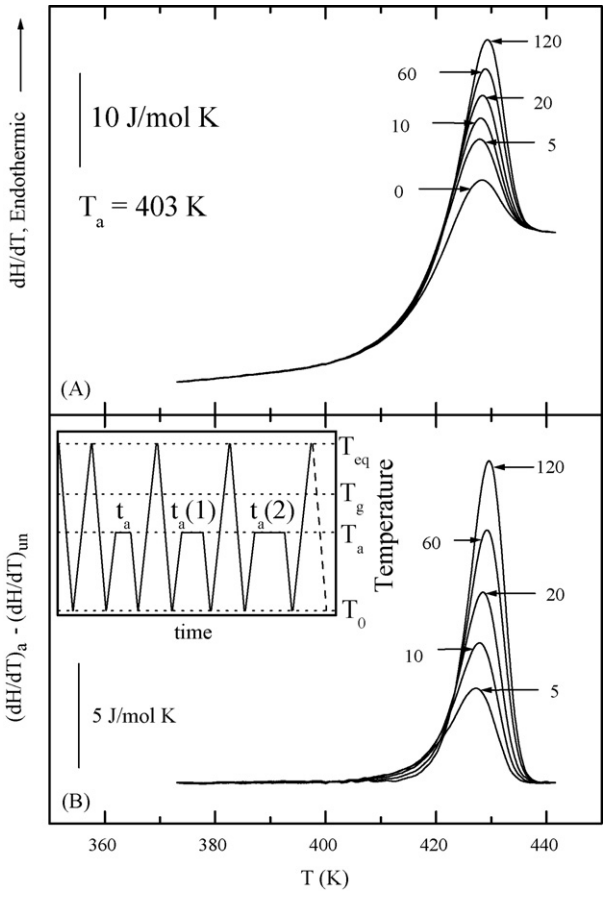

Fig. 2. (A) The dH/dT plots against the temperature obtained after isothermal annealing at 403 K for different annealing times. The numbers labeled to the curves refer to the annealing time in minutes. (B) The difference curves plotted against the temperature obtained by subtracting the DSC scan of the un-annealed sample (curve 0) from the DSC scan of the annealed samples. The numbers labeled to the curves refer to annealing times in minutes. Insert in (B) is an illustration of the procedure used for determining the relaxed values of the enthalpy and entropy, as described in Section 3.

times. From these scans, we obtained T_g of 414.2 K by the intersection point of two plots, one a tangent to the endothermic rise and the second an extension of the glass curve. The increase in the specific heat at T_g, ΔC_p, is 13.3 J/mol K for $Mg_{65}Cu_{25}Tb_{10}$ glass for q_h of 20 K/min.

To determine the decrease in enthalpy by structural relaxation during annealing (or storage) of a sample for different times, t_a, we use a procedure suggested by Lagasse [51], and used in previous studies [52–54]. It is illustrated in the insert in Fig. 2(B). In this procedure, an ultraviscous melt at a temperature, T_{eq}, is cooled at a (chosen) high rate, q_c, to a temperature, T_0, which is 75–80% of the calorimetric T_g. It is then heated at a chosen rate, q_h, from T_0 to T_{eq}. The DSC scan obtained on heating in this case is for the un-annealed sample, or for $t_a = 0$. The sample is then cooled from T_{eq} at the same rate, q_c, to T_0 and then heated at the fastest rate to the chosen annealing temperature, T_a, kept at T_a for a period of t_a minutes, cooled at the fastest rate to T_0, and then immediately heated to T_{eq} at rate q_h and its DSC scan obtained. This scan is for the sample annealed for t_a min at T_a. The procedure is repeated for different annealing periods, t_a (1), t_a (2), etc., for the same T_a. It is also then repeated but at different T_as. The sample is cooled back from T_{eq} to T_0 and then immediately heated at the fastest rate to a new T_a, say T_a (1), kept at T_a (1) for the same t_a as at the previous T_a. It is cooled back at the fast rate to T_0 and then finally heated to T_{eq} to obtain a new DSC scan. The procedure is repeated for a fixed t_a but for different T_a. The overall procedure is also then repeated, but by changing t_a.

It is required that all DSC scans whatever their annealing conditions should meet (i.e., have the same (dH/dt) value) at T_{eq}, and deviate only by an insignificant amount when the sample is deep in the glassy state. If the scans do not meet at T_{eq}, it would indicate that crystallization has occurred during the annealing, cooling and heating. Partial crystallization would reduce the (dH/dt) value much more at $T > T_{eq}$ than in the partial glassy state. DSC scans for different t_a at a fixed T_a of 403 K are presented in Fig. 2(A) and those at different T_a for a fixed t_a of 3 min are presented in Fig. 3(A). These clearly show no indication of crystallization. The scans also show that the usual procedure for obtaining T_g by intersection of the two lines, one extrapolated from the glass state and another drawn as a tangent at the point of inflexion of the sigmoid-shape curve would not yield the same T_g value, an aspect often overlooked in the DSC studies.

Typical plots for T_a of the glass at 403 K are shown in Fig. 2(A). The first scan for $t_a = 0$ min is labeled 0, and the scans obtained after annealing at 403 K for different t_as are labeled accordingly. The difference between the DSC scan at $t_a > 0$ and at $t_a = 0$, i.e., $[(dH/dT)_a - (dH/dT)_{un}]$ is plotted against T in Fig. 2(B) and is also labeled according to t_a. Similar experiments were performed for T_a of 363 K, 373 K, 383 K, and 393 K.

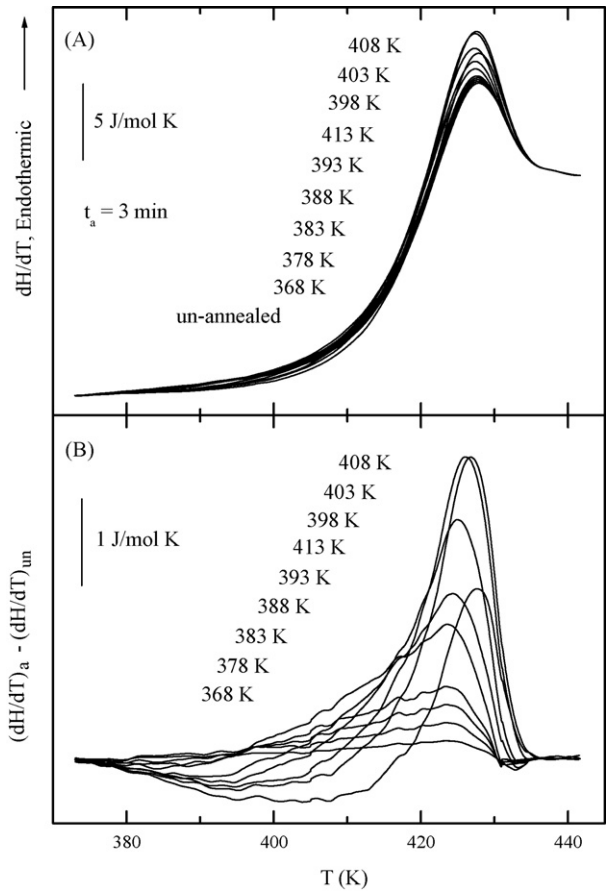

Fig. 3. (A) The dH/dT plots against the temperature obtained after isothermal annealing for 3 min at different annealing temperatures. The numbers shown refer to the annealing temperatures ordered according to the maximum of the curves. (B) The difference curves obtained by subtracting the DSC scan of the un-annealed sample from the DSC scan of the annealed samples. The numbers shown refer to the annealing temperatures ordered according to the maximum of the curves.

Typical plots for t_a of the glass for 3 min are shown in Fig. 3(A). The numbers shown refer to the annealing temperatures ordered according to the maximum of the curves. The difference curves between the un-annealed and annealed samples were obtained for each T_a and these are shown in Fig. 3(B). These also correspond to $[(dH/dT)_a - (dH/dT)_{un}]$ but for varying T_a. The numbers shown also refer to the annealing temperatures according to the order of ascending peak of the curves. Experiments were repeated for the set of (five) T_as but for t_a of 5 and 7 min.

4. Discussion

4.1. Isothermal structural relaxation of enthalpy and entropy

On isothermal structural relaxation H and S decrease with time, and density, frequency of vibrational modes, refractive index, and elastic modulus increase. The phenomenon studied at temperature not far below T_g is widely known as physical ageing in the polymer discipline and as annealing in the glass-making discipline. It is distinguished from another type of ageing that occurs at T far below T_g, such as the ageing of commercial silicate glasses at ambient temperature, whose density and refractive index also increase but by an almost imperceptible amount over a period of decades when a glass is kept at T of nearly half of its T_g, or lower. (For historical interest, we note that such ageing was first reported by James Prescott Joule who had observed that the zero temperature point of a gas thermometer made from a silicate glass shifted with time over a period of 38.5 years [55]. For details, a paper on silicate glasses [56] may be consulted where this ageing is shown to have a different mechanism than structural relaxation on physical ageing or on annealing.)

For analyzing the t, and T-dependence of H and S, we first use a general expression for the *irreversible* change and later use a phenomenological model used for molecular liquids [14], polymers [8] and inorganic melts [57]. The change in H is the sum of all the changes that occur during the cooling of a liquid, during the time of annealing and during the heating of a glass and are written as:

$$d\Delta H_a = \left(\frac{\partial \Delta H_a}{\partial t_a}\right)_{T_a,q_h,q_c} dt_a + \left(\frac{\partial \Delta H_a}{\partial T_a}\right)_{t_a,q_h,q_c} dT_a + \left(\frac{\partial \Delta H_a}{\partial q_c}\right)_{T_a,t_a,q_h} dq_c + \left(\frac{\partial \Delta H_a}{\partial q_h}\right)_{T_a,t_a,q_c} dq_h \quad (1)$$

where $d\Delta H_a$ is the difference between the enthalpy of the material before and after the annealing experiment, q_h is the heating rate, q_c the cooling rate, and other notations are as defined already. (Note that the derivatives imply change only in one direction, as is done in analyzing chemical kinetics equations and not in the usual thermodynamic equations.) The corresponding change in S is given by

$$d\Delta S_a = \left(\frac{\partial \Delta S_a}{\partial t_a}\right)_{T_a,q_h,q_c} dt_a + \left(\frac{\partial \Delta S_a}{\partial T_a}\right)_{t_a,q_h,q_c} dT_a + \left(\frac{\partial \Delta S_a}{\partial q_c}\right)_{T_a,t_a,q_h} dq_c + \left(\frac{\partial \Delta S_a}{\partial q_h}\right)_{T_a,t_a,q_c} dq_h \quad (2)$$

where the terms have the same meaning as in Eq. (1). The prefix Δ is used to maintain that the quantities determined by experiments are: $H - H(0\,K)$ and $S - S(0\,K)$, and not the absolute values of H and S. Thus Eqs. (1) and (2) include the effect of structural relaxation on the zero Kelvin values of the enthalpy and entropy. All four terms in Eqs. (1) and (2) are of practical significance because they describe the changes in the state of a glass when T fluctuates during its storage, and its rate varies. The first term was determined here from the plots in Fig. 2, and the second term from the plots in Fig. 3. Since q_c and q_h in both sets of experiments were 20 K/min, the magnitudes of the third and the fourth terms are zero.

4.2. Glass–liquid transition path and entropy

The spontaneity of structural relaxation makes the segment of the C_p path in the glass-softening range of its plot against T is irreversible in the sense that cooling and heating at the same rate do not yield the same values of C_p. Because of that, one may object to determining $d\Delta S_a$ from Eq. (2) here. Therefore, we first examine whether our analysis of the data to obtain $d\Delta S_a$ is valid, as follows:

We use the criteria that if C_p path is irreversible, the T_f determined from the $C_p\,d\ln T$ integral would be very different from the T_f determined from the $C_p dT$ integral. Therefore, if we analyze the same set of DSC data in two ways, and determine T_f^S from the $C_p d\ln T$ integral and T_f^H from the $C_p dT$ integral and find the two to be the same, our use of $C_p d\ln T$ integral would be justified. To do so, we determine the enthalpy change from the area between the curves, i.e., the $C_p dT$ integral from the plots in Fig. 1(B), as described by Moynihan et al. [58]

$$\int_T^{T_f'} (C_p^{liq} - C_p^{glass}) dT_f = \int_{T^*}^{T'} (C_p - C_p^{glass})\, dT \quad (3)$$

where T^* is any temperature above the transition region, C_p^{liq} is C_p of the liquid, T' is the temperature well below the glass transition

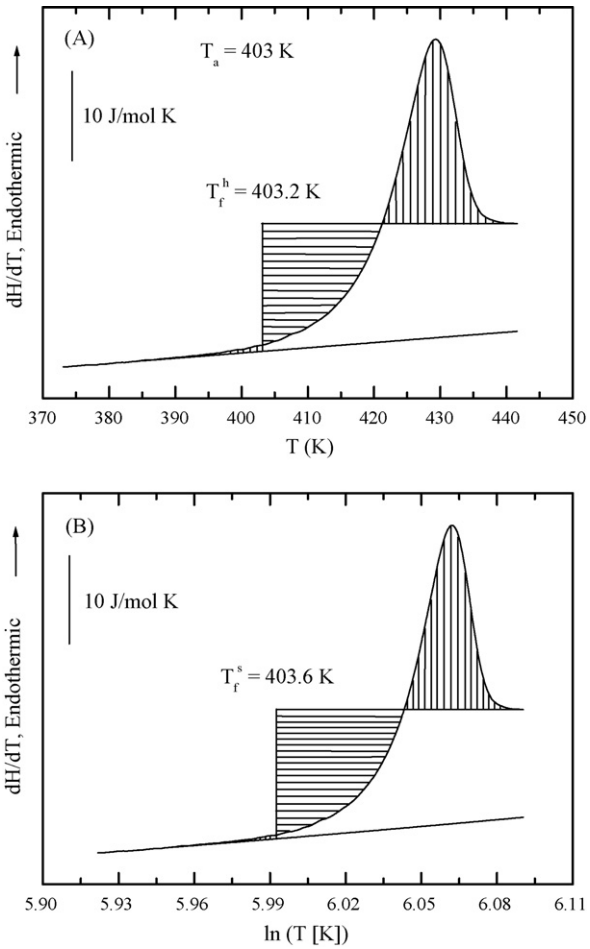

Fig. 4. (A) The plots of C_p against T for determining T_f^H by matching the area shown by vertical lines with the area shown by horizontal lines. The sample was cooled at 20 K/min from 443 K to 333 K, annealed for 120 min at 403 K and reheated at 20 K/min. (B) The same plots of C_p but against ln T for determining T_f^S by matching the area shown by vertical lines with the area shown by horizontal lines. Note that the $C_p dT$ integral yields the same T_f as the $C_p d\ln T$ integral.

region and C_p^{glass} is extrapolated C_p of the glassy state. C_p^{liq} is linearly extrapolated from the measured value and $T_f^{'}$ is the fictive temperature, which is noted here as T_f^H. Errors arising from this approximation are higher the longer is the extrapolation. Moynihan et al. had used DSC scans for q_h of 10 K/min, irrespective of q_c [58]. In the current literature, q_h of 20 K/min is used, because it is assumed that this rate yields T_g ($= T_f^H$) at which the structural relaxation time of the liquid is 100 s. (See Refs. [57,59] for its exceptions based on the width of the distribution.) Also, these quantities are determined by using the DSC scans on the premise that the ratio of the heat flow (in J s^{-1}) to q_h, $[(dH/dt)/q_h]$, is proportional to C_p of the glass, including the thermal effects of structural relaxation on C_p. From area matching according to Eq. (3) we determine T_f^H of 411.3 K from scans 1 and 2 in Fig. 1(B). Similarly, we determine T_f^H of 403.2 K for the sample that had been annealed for 120 min at 403 K from the plot in Fig. 2(A) by area matching shown graphically in Fig. 4(A). Note that both T_f^H values differ from the T_g of 414.2 K, that was obtained by the usual intersection method for scans 2 and 3 shown in Fig. 1(B).

To estimate T_f^S, we replace dT in Eq. (3) by d ln T to match the area for the entropy change

$$\int_{T}^{T_f'} (C_p^{liq} - C_p^{glass}) d\ \ln T_f = \int_{T^*}^{T'} (C_p - C_p^{glass}) d\ \ln T \quad (4)$$

Similar area matching in C_p against ln T curves based on Eq. (4) yields T_f^S as 403.6 K as is shown in Fig. 4(B) for the sample annealed for 120 min at 403 K. It is evident that T_f^S and T_f^H are the same within the experimental and analytical errors, and therefore we may use Eq. (2) for determining the net entropy change.

4.3. Enthalpy and entropy decrease on isothermal relaxation

The first and second coefficients in Eqs. (1) and (2) were determined from the area under the difference plots in Figs. 2(B) and 3(B). This yields the enthalpy regained on heating the annealed sample, which is equal to the enthalpy loss that occurred at a chosen T_a and t_a prior to heating. To determine the entropy loss on structural relaxation, the difference $[(dH/dT)_a - (dH/dT)_{un}]$ was plotted against ln T. The area under this plot gives the entropy regained on heating which is equal to the entropy lost on structural relaxation at a chosen T_a and t_a. If an exothermic dip-like feature also appeared prior to the broad peak in the difference curve, as seen in Fig. 3(B), the area of the dip was subtracted from the total area, i.e., a baseline at $dH/dT = 0$ was used to obtain $d\Delta H$ and $d\Delta S$. (This dip-like feature in the DSC scans of annealed samples is indication of a further enthalpy loss as a result of structural relaxation *during* the heating of the sample, which appears when T_a is such that the characteristic relaxation time is less than the value corresponding to $1/q_h$.)

The $d\Delta H_a$ thus determined from the data for T_a of 363 K, 373 K, 383K, 393 K, and 403 K in Fig. 2(B) is plotted as a negative quantity against t_a in Fig. 5(A). The corresponding $-d\Delta S_a$ is plotted against t_a in Fig. 5(B). Similarly, $d\Delta H_a$ and $d\Delta S_a$ at different T_a and fixed t_a were obtained from the data in Fig. 3. The $-d\Delta H_a$ is plotted against T_a in Fig. 6(A) for each set of t_a of 3 min, 5 min and 7 min,

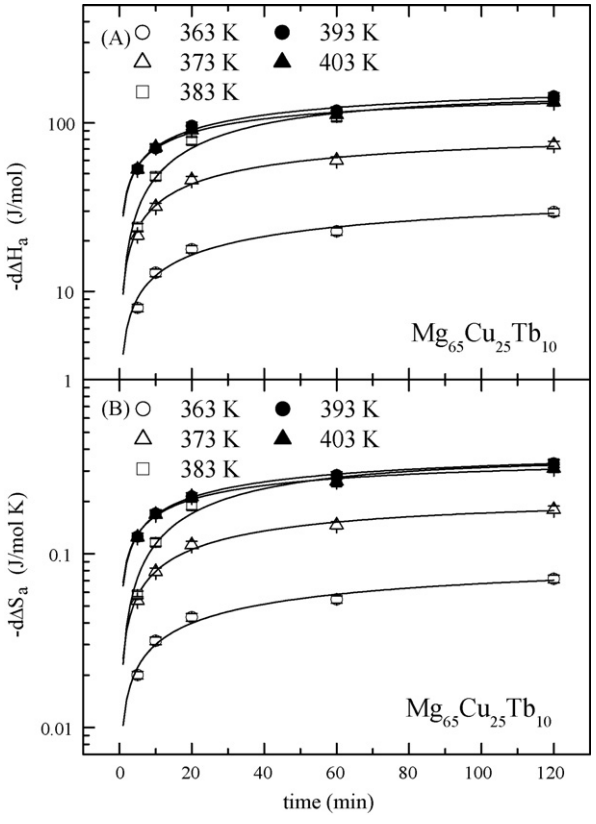

Fig. 5. The enthalpy and entropy loss are plotted against the annealing time during isothermal annealing of $Mg_{65}Cu_{25}Tb_{10}$ metal alloy glass at annealing temperature of 363 K, 373 K, 383 K, 393 K, and 403 K.

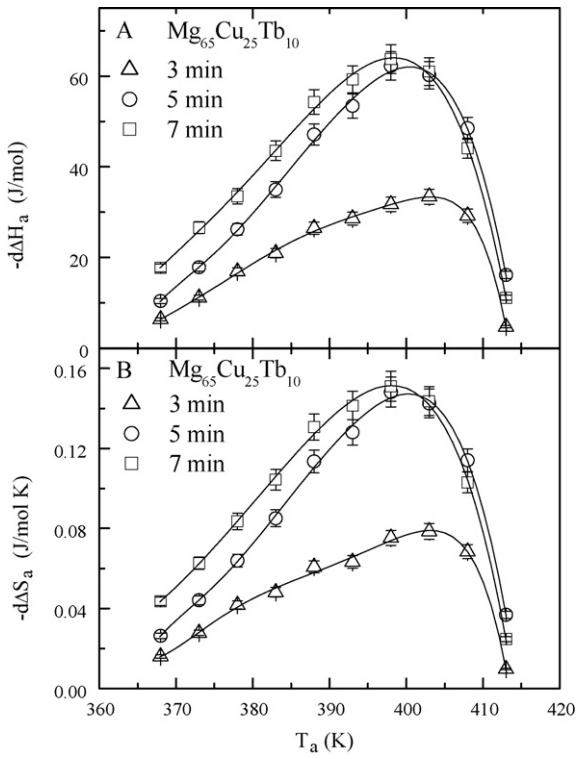

Fig. 6. The enthalpy and entropy loss are plotted against annealing temperature during isothermal annealing of $Mg_{65}Cu_{25}Tb_{10}$ metal alloy glass for the annealing time of 3, 5, and 7 min.

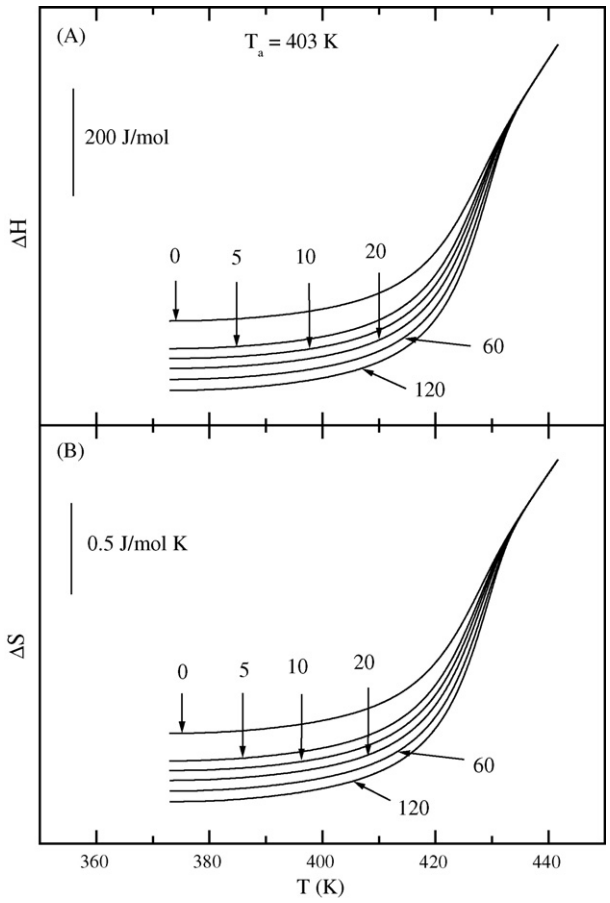

Fig. 7. The enthalpy and entropy loss of $Mg_{65}Cu_{25}Tb_{10}$ metal alloy glass after isothermal annealing at 403 K for different annealing times are plotted against the temperature. The numbers labeled to the curves refer to the annealing time in minutes.

as is indicated. The corresponding plots of $-d\Delta S_a$ are shown in Fig. 6(B). The $-d\Delta H_a$ and $-d\Delta S_a$ values include the decrease in the enthalpy at 0 K, as well as that in the residual entropy, S_{res} (the value at absolute zero temperature) that occurs on annealing the glass.

4.4. Relaxation of ΔH and ΔS with time and temperature

We now determine the change in H and S on heating a glass by using the relations

$$\Delta H(T) = \Delta H(T_a) + \int_{T_a}^{T} (C_p^a - C_p^{un})dT \quad (5)$$

$$\Delta S(T) = \Delta S(T_a) + \int_{T_a}^{T} (C_p^a - C_p^{un})d\ \ln T \quad (6)$$

where $\Delta H(T_a)$ and $\Delta S(T_a)$ are the total decrease that occurs on annealing at T_a and the integral term adds to their negative values. Since H and S of a liquid are state functions, the plots of $\Delta H(T)$ and $\Delta S(T)$ against T for all t_a and T_a conditions would merge when liquid state is reached on heating. Since such plots are useful in determining both the relative change in H and S with T and the manner of the change, we calculated $\Delta H(T)$ and $\Delta S(T)$ from Eqs. (5) and (6) by using the data from Figs. 2 and 3 and have plotted these against T in Fig. 7(A) and (B) for T_a of 403 K. The curve labeled 0 is for the un-annealed sample and other curves for t_a of 5, 10, 20, 60, and 120 min are as labeled. The corresponding plots for the second set of experiment for fixed t_a and varying T_a are presented in Fig. 8. The un-annealed sample curve is as labeled and the numbers shown refers to the ascending T_a for other curves.

We analyze our results first by using the simplest kinetic equations

$$\partial\Delta H_a(t_a, T_a) = [\Delta H(t_a = 0, T_a) - \Delta H(t_a \to \infty, T_a)] \times \left[1 - \exp\left\{-\left(\frac{t_a}{\tau(T_a)}\right)^{\beta}\right\}\right] \quad (7)$$

$$\partial\Delta S_a(t_a, T_a) = [\Delta S(t_a = 0, T_a) - \Delta S(t_a \to \infty, T_a)] \times \left[1 - \exp\left\{-\left(\frac{t_a}{\tau(T_a)}\right)^{\beta}\right\}\right] \quad (8)$$

where β is a fitting parameter, which is equal to 1, for an exponential process and τ the characteristic time for structural relaxation, which in this model is assumed to be given by the Arrhenius relation, $\tau = \tau_{0,A} \exp(E_A^*/RT_a)$, with $\tau_{0,A}$ as the pre-exponential factor, E_A^* the Arrhenius activation energy and R the gas constant. Eqs. (7) and (8) were fitted to the data in the plots of $d\Delta H_a$ and $d\Delta S_a$ against t_a in Fig. 5. Best-fit of Eq. (7) to the data for the glass annealed at 403 K in Fig. 5(A) yields, $\Delta H(t_a = 0, T_a) - \Delta H(t_a \to \infty, T_a) = 152$ J/mol, $\tau = 27.42$ min and $\beta = 0.47$. The corresponding fit of Eq. (8) to the data in Fig. 5(B) yields, $\Delta S(t_a = 0, T_a) - \Delta S(t_a \to \infty, T_a) = 0.36$ J/mol K, $\tau = 27.42$ min and $\beta = 0.47$.

The second term on RHS of Eq. (1) and (2) quantifies the effect of T_a, and it is determined also from the areas under the peaks in the plots in Fig. 2(B) and the plots against $\ln T$ (not shown). When the glass was annealed at selected T_as for a fixed period, $-d\Delta H_a$ and $-d\Delta S_a$ reached a maximum value as is seen in Fig. 6. This results

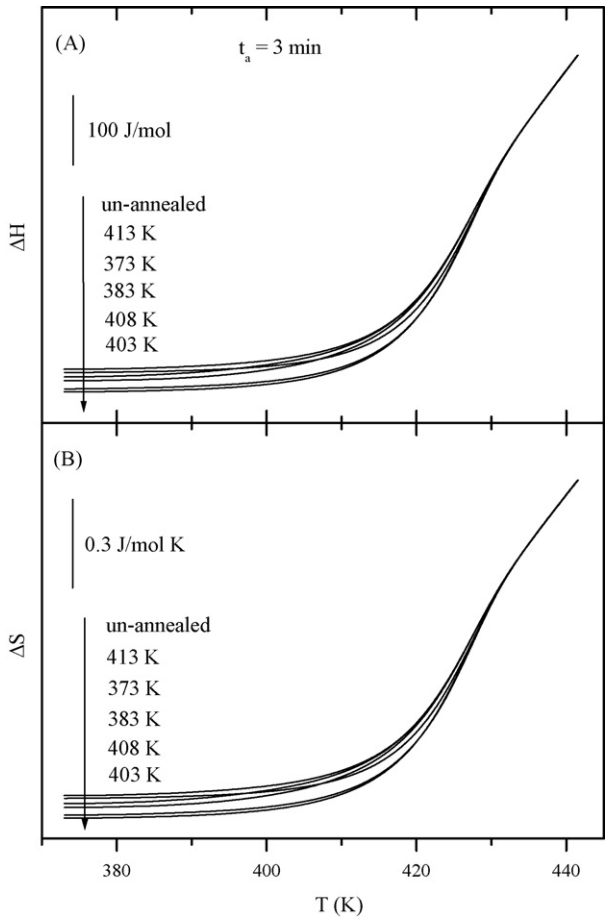

Fig. 8. The enthalpy and entropy loss of $Mg_{65}Cu_{25}Tb_{10}$ metal alloy glass is plotted against the temperature after isothermal annealing for 3 min at different annealing temperatures. The numbers shown refer to the annealing temperatures ordered according to the left edge of the curves.

from two competing effects: the first dominates at low T_a at which τ is long and the decrease in $d\Delta H_a$ and $d\Delta S_a$ over a fixed t_a is initially too small to be measurable and as τ decreases rapidly when T_a is increased and $-d\Delta H_a$ and $-d\Delta S_a$ increase. The second dominates when T_a is high, structural relaxation is near completion in the fixed t_a and the magnitudes of $[\Delta H(t_a = 0, T_a) - \Delta H(t_a = \infty, T_a)]$ and $[\Delta S(t_a = 0, T_a) - \Delta S(t_a = \infty, T_a)]$ decrease as T_a is increased. Thus the shape of the plot in Fig. 6 is determined by, (i) a kinetically limiting process that increases the spontaneous loss of H and S as T_a is increased and t_a is kept fixed, and (ii) a thermodynamic limiting difference between the initial and ultimate values of H and S as T_a is increased. The peaks in $d\Delta H_a$ and $d\Delta S_a$ appear at a T_a when effect (ii) begins to dominate. Formally, for a fixed t_a and varying T_a, conditions for which $d\Delta H_a$ and $d\Delta S_a$ reach their peak value (at T_{peak}) are given by

$$-\frac{\partial \ln\ \Delta H_a(T_a)}{\partial T_a} = \frac{\beta t_a^{\beta} E_A^*}{\tau(T_a)^{\beta} R T_{peak}^2} \tag{9}$$

$$-\frac{\partial \ln\ \Delta S_a(T_a)}{\partial T_a} = \frac{\beta t_a^{\beta} E_A^*}{\tau(T_a)^{\beta} R T_{peak}^2} \tag{10}$$

and by rearranging the equations above

$$T_{peak} = \left(\frac{\beta t_a^{\beta} E_A^*}{-\tau(T_a)^{\beta} R[\partial \ln\ \Delta H_a(T_a)/\partial T_a)]} \right)^{1/2} \tag{11}$$

$$T_{peak} = \left(\frac{\beta t_a^{\beta} E_A^*}{-\tau(T_a)^{\beta} R[\partial \ln\ \Delta S_a(T_a)/\partial T_a)]} \right)^{1/2} \tag{12}$$

Because of lack of data we do not use Eqs. (11) and (12) here. These are included for completion and their validity may be tested when more extensive data become available.

It should be noted that Eqs. (7) and (8) are intended for direct analysis rather than model fitting to a DSC scan, and these would not be useful for describing the non-linearity effects resulting from the structure dependence of the relaxation times. As discussed later here, inclusion of the effects in model calculations also does not lead to satisfactory results.

4.5. Molecular processes and structural relaxation

In 1937, Bernal [60] had concluded that C_p^{liq} varies with T partly due to change in the liquid's structure and partly due to change in the molecular vibrational frequency. The change in the H and S observed on heating a glass are therefore attributable to an increase in the configurational and vibrational contributions at a fixed T. The decrease in H and S on structural relaxation at a fixed T_a is therefore due to attainment of configurationally low energy state as well as vibrationally different, less anharmonic (low-energy) state of lower C_p. On heating a glass, the configurational and vibrational contributions decrease due to structural relaxation, and increase with increase in T. The first dominates initially and the second dominates in the later stage and their rates cancel out at T where the peak appears in the plots in Fig. 6(A) and (B). While the physical origins of the two effects are common to all glasses, the vibrational contribution is usually ignored, even though it is significant because configurational states of high energy also have low vibrational frequencies and hence a large vibrational contribution.

For a metal–alloy glass, there is also an entropy of mixing that is a part of the configurational entropy, and both would change in the case any short range ordering of the structure, and both would kinetically freeze on cooling at the same temperature and unfreeze on heating. The maximum entropy of mixing for this glass is equal to $-R\sum_i x_i \ln x_i$, where R is the gas constant and x_i is the mole fraction of the component i. Its value for $Mg_{65}Cu_{25}Tb_{10}$ glass is 7.12 J mol^{-1} K^{-1}.

4.6. Description in terms of a non-exponential non-linear model

A variety of models have been developed for fitting to the DSC scans, and all of these admit to a phenomenology that is based upon the original observations of Winter-Klein [61] and Tool [15] and a mathematical treatment introduced by Narayanaswamy [62]. The model was applied to the DSC scans of molecular liquids and polymers originally by Moynihan et al. [14], and an algorithm for fitting to the DSC scan was developed by Hodge and Berens [63] who used it to simulate the DSC scans for amorphous polymers. To examine the validity of such models, we fit the Tool–Narayanaswamy–Moynihan formalism to our DSC data. Accordingly [12,62,63],

$$\tau = A \exp\left[\frac{x\Delta h^*}{RT} + \frac{(1-x)\Delta h^*}{RT_f}\right] \tag{13}$$

where τ is the characteristic relaxation time, Δh^* is the activation energy, A is a parameter equal to τ when both T and T_f are formally infinity, and x is an empirical parameter referred to as the non-linearity parameter, whose value is between 0 and 1. The normalized relaxation function is written as, $\phi = \exp[-(t/\tau)^{\beta}]$, where β is the stretched exponential parameter and t is the macroscopic time. Details of data fitting may be found in Refs. [54,57].

Briefly, the DSC data were transformed into a normalized heat capacity

$$C_{\mathrm{p,norm}} = \left(\frac{C_{\mathrm{p,meas}}(T) - C_{\mathrm{p}}^{\mathrm{glass}}(T)}{C_{\mathrm{p}}^{\mathrm{liq}}(T) - C_{\mathrm{p}}^{\mathrm{glass}}(T)} \right) \quad (14)$$

where $C_{\mathrm{p,meas}}(T)$ is taken as the measured $(\mathrm{d}H/\mathrm{d}t)$ in a DSC scan divided by $q_{\mathrm{h}} = \mathrm{d}T/\mathrm{d}t$. Fig. 9 shows the normalized DSC scans obtained for un-annealed and annealed $Mg_{65}Cu_{25}Tb_{10}$ glass. The fit to these scans was obtained with a least squares Marquardt algorithm by using temperature step of 0.5 K, and annealing time step of at least 1 s (for $t > 2$ ks, the annealing time step was equal to $t_{\mathrm{n}}/2000$). The best-fit parameters obtained for sample annealed for 10 min are: $\ln A = -118$, $x = 0.47$, $\beta = 0.60$, $\Delta h^* = 423$ kJ/mol, and the simulated scans are shown by dash-dot lines. These parameters are expected to describe the curves for all annealing conditions, but Fig. 9 shows that a good fit is obtained only for the sample annealed for 10 min. The fit is satisfactory for the un-annealed sample and less so for the 5 min annealed sample, it is quite unsatisfactory for the 20 min, 60 min and 120 min annealed samples. The discrepancy indicates limitations of the model in predicting the consequences of structural relaxation on annealing over a long time period.

To express the fit of the equations to the experimental data in an alternative manner, we have calculated the relaxation time, τ, from the simulated plots in Fig. 9. It is plotted logarithmically (to the base 10) against $1/T$ in Fig. 10(A), and for clarity against T in Fig. 10(B). The plot in Fig. 10(A) is non-linear at T up to 10 K below

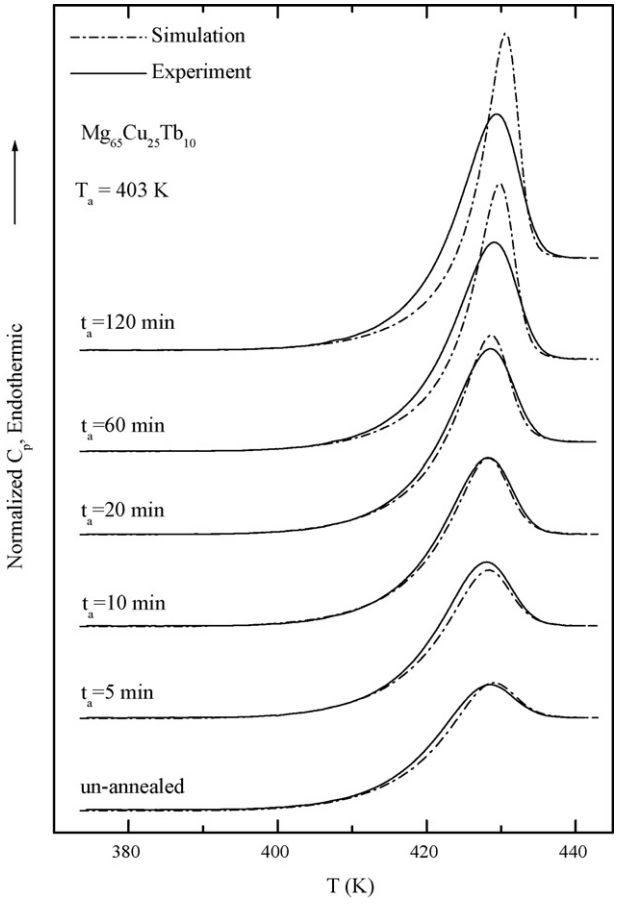

Fig. 9. The TNM simulation of heating curves after isothermal annealing at 403 K for different annealing times. The parameters for simulation are $\ln A = -118$, $x = 0.47$, $\beta = 0.60$, $\Delta h^* = 423$ kJ/mol.

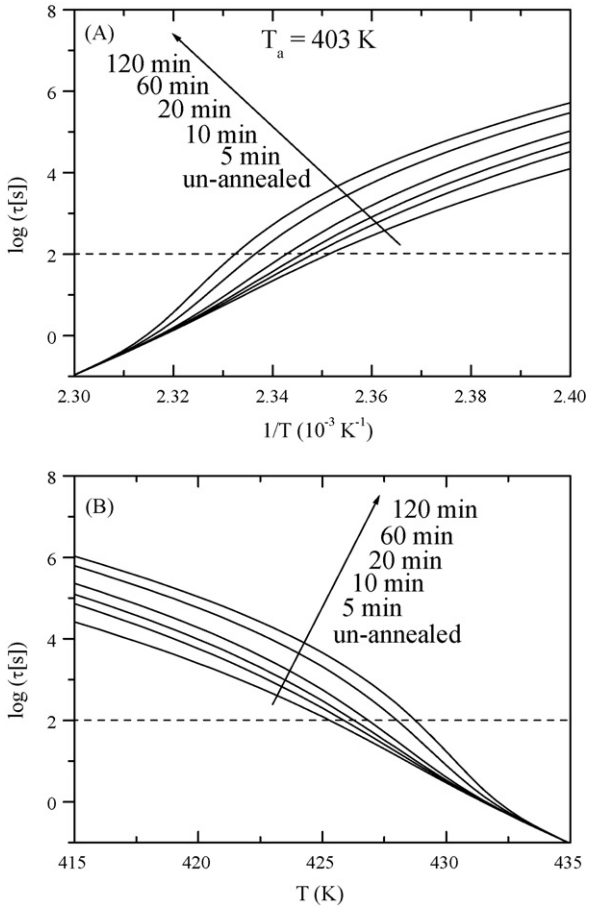

Fig. 10. The plots of the calculated relaxation time from the fitted curves in Fig. 9. (A) Plots against $1/T$. (B) Plots against T.

T_{g}, and is expected to become linear at lower temperatures when the effect of distribution of times is reduced. This is a characteristic of an Arrhenius temperature dependence and is expected from Eq. (13) when $T = T_{\mathrm{f}}^{\mathrm{H}}$ in the equilibrium state.

Also τ for the annealed sample cannot be reliably estimated when the fit-parameters for un-annealed sample are used. In summary, the fit parameters for the annealed samples in Fig. 9 do not yield reliable value for the enthalpy regain on heating the annealed sample. For that reason, Eqs. (1), (2), (6) and (7) seems to be a better description of structural relaxation, than a structural relaxation model. There seems to be no independent manner of determining τ from the DSC data to ascertain if the calculations yield the correct value of τ, but modulated calorimetry data provide such values [64–66]. Nevertheless, they show that the structural relaxation of the glass has a broad distribution also of atomic diffusion time.

The poor fit of the model to the data may also be due to the approximations made in developing and using these models, which we briefly note below:

(i) For calculating $C_{\mathrm{p,norm}}$ from Eq. (14) one uses linear extrapolation of $C_{\mathrm{p}}^{\mathrm{liq}}$ from $T \gg T_{\mathrm{g}}$ to $T \ll T_{\mathrm{g}}$, and of $C_{\mathrm{p}}^{\mathrm{glass}}$ from $T \ll T_{\mathrm{g}}$ to $T \gg T_{\mathrm{g}}$. But $C_{\mathrm{p}}^{\mathrm{glass}}$ itself increases non-linearly with T because contributions from anharmonic forces of the potential function and from β-relaxation configurations (also known as the JG relaxation) increase rapidly with increase in T. As a result, the slope of $C_{\mathrm{p}}^{\mathrm{glass}}$ against T plot increases as T_{g} is approached on heating and linear extrapolation becomes questionable. Also,

plots of C_p^{liq} against T for ultraviscous liquids at $T > T_g$ are curved, and either $C_p^{liq}/dT < 0$, as for 1-butene an N-type liquid, or $(dC_p^{liq}/dT) > 0$, as for *o*-terphenyl, a P-type liquid. For metallic glasses, the high temperature data are insufficient for C_p^{liq} extrapolation.

(ii) The quantity dT_f^H/dT of liquid is taken to be equal to 1. This means that, on extrapolation, T_f^H would reach zero at $T > 0$ K. By extrapolating a supercooled liquid's entropy to $T < T_g$, Kauzmann [67] had suggested that its entropy may become equal to that of a crystal at a temperature T_K. The Adam–Gibbs theory [12] that relies on the Kauzmann extrapolation but instead of the excess entropy S_{exc} of the liquid over the crystal phase, uses the configurational entropy S_{conf} that is zero at T_K or T_2, even though $S_{conf} < S_{exc}$. As an alternative to Kauzmann and Adam–Gibbs extrapolations, interpolation of C_p between 0 K and T_g has been suggested [68,69] following the argument given by Simon [70]. In this interpolation, S_{exc} tends to zero at 0 K. An analysis of the C_p data of amorphous polyethylene provide support for the absence of the T_K or T_2 [71], and an analysis of the DSC data on a polymer [72] has suggested a similar absence of T_K. (Note that extra contributions from anharmonic forces [68,73,74], and from motion of atoms or molecules occupying higher volume sites in the glass structure would not allow S_{exc} to become zero at T_K.) In summary, dT_f^H/dT would not approach zero at $T > 0$ K. Rather it would decrease slowly from its value of 1 to zero at 0 K. The plot of T_f^H against T therefore would be curved and would flatten out as $T \to 0$ K. Our study further shows that T_f^S against T plot would also be curved and would flatten out as $T \to 0$ K.

(iii) The parameter β is assumed to remain constant with t_a, T and T_a, although it is acknowledged that β is expected to change. The studies here and earlier [53,74–77] show that β changes, thus confirming Douglass's 1966 finding [78] that β changes with t_a.

(iv) It is assumed that there is no contribution to C_p from the increasing strength of the JG relaxation on heating a glass.

Nevertheless, these models are found to be adequate for fitting a DSC scan over a narrow temperature range, implying that the combined effects of the above-given approximations are insignificant in comparison with the experimental errors. The parameters obtained are useful for a self-consistent analysis of the DSC data. If the above-given effects were to be included, it would add to adjustable parameters.We also note that Fig. 5 provides a direct analysis of the data on time dependence of the enthalpy and entropy change at fixed T_a. This is in contrast to the normalized C_p change observed on heating when the TNM model is fitted to a DSC scan and the two cannot be compared. Also, in their studies, Hodge and Berens [63] used a temperature-step of 1 K for all simulations of the TNM model and found it to be satisfactory. We have used the step as 0.5 K for greater accuracy and yet we have found large differences between the measured and simulated DSC scans here for annealed samples, as also in earlier studies [54].

4.7. Endothermic relaxation in the glassy state

When the structure of a solid does not change with t or T, C_p or (dH/dT) increases on heating. But, when its structure relaxes C_p decreases, and its DSC scan shows first a broad minimum at $T < T_g$ and thereafter a rise in (dH/dT) toward the liquid state value. When an already highly annealed glass is heated, the (dH/dT) does not show a minimum. One sample of $Mg_{65}Cu_{25}Tb_{10}$ in this study had been kept for a period (unknown) of more than 6 months at ambient temperature before its scan 1 shown in Fig. 1(B) was obtained. The scan shows no decrease below the (dH/dT) for the glass, as ascertained by its rescan in Fig. 2. Instead it shows an endothermic rise in (dH/dT) followed by a decrease and finally a second endothermic rise in the glass-softening range of 420–440 K. An apparently similar feature has been observed for several other metal-alloy glasses [43,79], but in those studies a deep exotherm appears after the endothermic peak, and C_p of the annealed and the (un-annealed) quenched sample at higher T have the same value. It was also found that when a glass formed by slow cooling is annealed, it shows an endothermic peak and thereafter C_p decreases to the value for the un-annealed sample and the two values remain the same until C_p^{liq} has been reached and in this respect, the feature seen in Fig. 1(B) differs from the known features. For metal–alloy glasses it was interpreted to indicate that "the relaxation entities responsible for the short relaxation times are operating more or less independently from each other while the long time relaxation process which occurs near T_g is cooperative in nature" [79]. The two processes were seen to arise "from a single continuous relaxation spectrum and it was proposed that the structure of ultraviscous liquid is inhomogenous and hence the glass transition was treated as a percolation process" [79]. In more recent discussion of metal–alloy glasses similar features have been attributed to the onset of the JG relaxation [80].

For a further analysis, we plot the difference between scan 1 and 2 against T in Fig. 1(C). It indicates that if there were an exothermic effect, it has been overwhelmed by the low temperature endotherm. In the period of several months at ambient temperature, the glass structure became highly relaxed even though it was prepared originally by relatively slow cooling. In earlier studies where the effect of the distribution of relaxation times was investigated in the glassy state [22,23], several metal–alloy glasses were cooled from $T < T_g$, annealed and then heated back to the same $T < T_g$, i.e., thermally cycled in a T range below T_g, a similar but much smaller endothermic peak was observed. That endothermic peak was attributed to the unfreezing of the faster relaxation modes in the distribution of the main or the α-relaxation process. If JG relaxation occurs at a rate comparable to these faster modes, its own strength would decrease on annealing, as is already known [81–84], and would be recovered on heating the glass. The recovery would appear as an overshoot of the type usually observed at $T > T_g$ and attributed to the α-relaxation. But when the rate of the JG relaxation is close to that of the α-relaxation or they appear at temperatures relatively close to each other, recovery of the of the JG relaxation configurations would be accompanied by the recovery of the faster modes in a distribution of the α-relaxation contributions. Thus the JG relaxation in a DSC scan can be distinguished only if its relaxation rate is much faster than that of the faster modes of the α-relaxation and its magnitude relatively large.

Ichitsubo et al. [85–87] have found evidence for inter-dispersed regions of low and high densities in the structure of a glass. Thus they envisaged the structure of a glass as a composite of weakly bonded and strongly bonded regions. By studying accelerated crystallization caused by high-energy ultrasonic waves traveling through metal alloy glasses, they deduced that atoms in the weakly bonded regions or "islands of mobility" in the glass structure have a lower vibrational frequency. As these regions do not resist a shear stress, they argued that when the volume fraction of such regions is large their Poisson's ratio is large. Since annealing decreases the fractional population of such regions, it would decrease the Poisson's ratio.

We envisage that when the majority of the atoms in a glass structure at $T < T_g$ are kinetically frozen-in, the rapid approach towards an equilibrium of a small, but increasing number of locally diffusing atoms produces a small overshoot at a temperature determined by its diffusion rate and the rate of heating. In this view, the endother-

mic peak observed on heating an annealed glass is a reflection of the sum of a multitude of C_p overshoots, each corresponding to a "mini glass–liquid transition" of the localized groups of atoms. Superposed on it is the recovery of configurations of atoms in local regions that produce a JG relaxation without causing the glass to show viscous flow over a short period. The entropy of mixing of 7.12 J mol^{-1} K^{-1} would also unfreeze on heating to the liquid state, and some of it may also unfreeze at a lower T where JG relaxation within the localized group of atoms unfreezes at $T < T_g$. The fraction of that entropy loss would be relatively small. This contribution is absent in a mono-component glass.

5. Conclusions

Isothermal structural relaxation of $Mg_{65}Cu_{25}Tb_{10}$ glass, in which atomic diffusion determines the kinetics, follows a stretched exponential relation with a parameter that remains constant with the annealing time. For the same annealing period at different annealing temperatures, the decrease in H and S shows a peak as the sample reaches an equilibrium state for that annealing period.

The fictive temperature estimated from the $C_p dT$ integral is the same as that estimated from the $C_p d\ln T$ integral. The non-exponential, non-linear enthalpy relaxation model fits the heating DSC scan data for structurally unrelaxed sample, but not for the relaxed samples, i.e., a single set of parameters does not describe the behavior on heating of a highly structurally relaxed $Mg_{65}Cu_{25}Tb_{10}$ glass, and the non-exponential parameter is less than that determined from isothermal structural relaxation.

$Mg_{65}Cu_{25}Tb_{10}$ glass stored at ambient conditions shows an endothermic peak in dH/dT on heating at $T < T_g$ and the usual dH/dT overshoot at $T > T_g$. This peak is due partly to the unfreezing of the JG relaxation in the glassy state and partly to the unfreezing of the faster modes in the distribution of the α-relaxation times. It may be seen as the sum of a multitude of 'overshoots' in the apparent C_p still in the glassy state, and to correspond to localized motions when localized group of atoms kinetic unfreeze. This is qualitatively similar to the overshoot observed in a DSC heating scan. This is one aspect of the distribution of diffusion times in local regions that arises from spatial and temporal distinctions of the atomic environment in the structure of a glass. Similarity of the structural relaxation effects with polymers and other glasses show that thermodynamics and kinetics provides no distinction between the changes in the topological and chemical short range orders in the metal alloy glass.

Acknowledgment

This research was supported by a Discovery Grant from Natural Sciences and Engineering Research Council of Canada.

References

[1] R.O. Davies, G.O. Jones, R.O. Davies, G.O. Jones, Adv. Phys. 2 (1953) 370.
[2] G.W. Scherer, Relaxation in Glass and Composites, John Wiley, 1986.
[3] I. Gutzow, J. Schmelzer, The Vitreous State: Thermodynamics, Structure, Rheology and Crystallization, Springer, Heidelberg, 1995.
[4] S.V. Nemilov, Thermodynamics and Kinetic Aspects of the Vitreous State, CRC, Boca Raton, FL, 1995.
[5] J. Perez, Physique et mecanique des polymeres amorphes, Lavoisier, Tec & Doc, Paris, 1992.
[6] A.J. Kovacs, Fortschr. Hochpolym. Forsch. (Adv. Polym. Sci.) 3 (1963) 394.
[7] A.J. Kovacs, J.J. Aklonis, J.M. Hutchinson, A.R. Ramos, J. Polym. Sci. Polym. Phys. 17 (1979) 1097.
[8] I.M. Hodge, J. Non-Cryst. Solids 169 (1994) 211.
[9] K. Adachi, K. Kotaka, Polym. J. 14 (1982) 959.
[10] J.M. O'Reilly, Critical Reviews in Solid State and Materials Science, vol. 13, CRC, Boca Raton, FL, 1987, pp. 259–227.
[11] G.B. McKenna, in: C. Booth, C. Price (Eds.), Comprehensive Polymer Science, vol. 2, Pergamon, Oxford, 1989, p. 311 (Chapter 10).
[12] G. Adam, J.H. Gibbs, J. Chem. Phys. 43 (1965) 139.
[13] M.H. Cohen, D. Turnbull, J. Chem. Phys. 31 (1959) 1164.
[14] C.T. Moynihan, P.B. Macedo, C.J. Montrose, P.K. Gupta, M.A. Debolt, J.F. Dill, B.E. Dom, P.W. Drake, A.J. Easteal, P.B. Eltermann, R.A. Moeller, H. Sasabe, J.A. Wilder, Ann. N. Y. Acad. Sci. 279 (1976) 15.
[15] Q. Tool, J. Am. Ceram. Soc. 29 (1946) 240.
[16] A. Inoue, T. Zhang, T. Matsumoto, Mater. Trans. JIM 30 (1989) 965.
[17] A. Peker, W.L. Johnson, Appl. Phys. Lett. 63 (1993) 2342.
[18] W.H. Wang, C. Dong, C.H. Shek, Mater. Sci. Eng. R44 (2004) 45.
[19] D.P.B. Aji, P. Wen, G.P. Johari, J. Non-Cryst. Solids 353 (2007) 3796.
[20] T. Egami, J. Mater. Sci. 13 (1978) 2587, SRO and CRO.
[21] T. Egami, in: P. Haasen, R.I. Jaffe (Eds.), Amorphous Metals and Semiconductors, Pegamon, Oxford, 1986, p. 22.
[22] J.G. Shim, G.P. Johari, Philos. Mag. B 79 (1999) 565–584.
[23] G.P. Johari, J.G. Shim, J. Non-Cryst. Solids 261 (2000) 52–66.
[24] H.S. Chen, J. Appl. Phys. 52 (1981) 1868.
[25] H.S. Chen, J. Non-Cryst. Solids 27 (1978) 257.
[26] M.G. Scott, A. Kursumovic, R.W. Cahn, Scripta Metall. 14 (1980) 1245.
[27] M.G. Scott, A. Kursumovic, Appl. Phys. Lett. 37 (1980) 620.
[28] M.G. Scott, A. Kursumovic, E. Gritt, R.W. Cahn, Scripta Metall. 14 (1980) 1303.
[29] B.S. Berry, W.C. Pritchet, J. Appl. Phys. 44 (1973) 3122.
[30] B.S. Berry, W.C. Pritchet, Scripta Metall. 15 (1981) 637.
[31] T. Egami, R.S. Williams, IEEE Trans. Magn. MAG-12 (1976) 927.
[32] T. Egami, T. Ichikawa, Mater. Sci. Eng. 32 (1978) 293.
[33] T. Egami, J. Mater. Sci. 13 (1978) 2587.
[34] T. Egami, T. Kudo, in: T. Masumoto, K. Suzuki (Eds.), Proceedings of the 4th International Conference on Rapidly Quenched Metals, Japan Institute of Metals, Sendai, 1982.
[35] A.I. Taub, F. Spaepen, Acta Metall. 28 (1980) 1781.
[36] A.I. Taub, F.E. Luborsky, Acta Metall. 29 (1981) 1939.
[37] G.P. Johari, R.J. Wang, W.H. Wang, Phys. Rev. B 73 (2006) 224203.
[38] G.P. Johari, Philos. Mag. 86 (2006) 1567.
[39] G.P. Tiwari, R.V. Ramanujan, M.R. Gonal, R. Prasad, P. Raj, B.P. Badguzar, G.L. Goswami, Mater. Sci. Eng. A 304–306 (2001) 499.
[40] T. Egami, Mater. Res. Bull. 13 (1977) 557.
[41] S.R. Elliot, Physics of Amorphous Materials, Pergamon, Oxgord, 1983, p. 222.
[42] A. Van den Beukel, S. Radelaar, Acta Metall. 30 (1983) 419.
[43] A. Inoue, T. Masumoto, H.S. Chen, J. Mater. Sci. 19 (1984) 3953.
[44] H.S. Chen, A. Inoue, J. Non-Cryst. Solids 61–62 (1984) 805.
[45] W.H. Wang, Z.H. Zhao, Z. Zhang, P. Wen, M.X. Pan, D.Q. Zhao, W.L. Wang, Appl. Phys. Lett. 82 (2003) 4699.
[46] W.H. Wang, X.K. Xi, D.Q. Zhao, M.X. Pan, Intermetallics 13 (2005) 638.
[47] W.H. Wang, Z.F. Zhao, P. Wen, R.J. Wang, D.Q. Zhao, M.X. Pan, J. Mater. Res. 21 (2006) 369.
[48] W.H. Wang, L.M. Wang, L.L. Sun, J. Zhang, W.K. Wang, Phys. Rev. B 63 (2001) 052210.
[49] W.H. Wang, L.M. Wang, R.J. Wang, L.L. Sun, W.K. Wang, J. Phys. Condens. Mater 15 (2003) 101.
[50] W.H. Wang, X.K. Xi, D.Q. Zhao, M.X. Pan, Y. Wu, J.J. Lewandowski, Phys. Rev. Lett. 94 (2005) 125510.
[51] R.R. Lagasse, J. Polym. Sci. Polym. Phys. 20 (1982) 279.
[52] S. Rüdisser, A. Hallbrucker, E. Mayer, G.P. Johari, J. Phys. Chem. 101 (1997) 266.
[53] A. Fransson, G. Backstrom, Int. J. Thermophys. 8 (1987) 352.
[54] L. Gunawan, G.P. Johari, R.M. Shanker, Pharm. Res. 23 (2006) 967.
[55] J.P. Joule, Observations on the Alteration of the Freezing-point in Thermometers. Scientific Papers of James Prescott Joule, vol. I, The Physical Society of London, Taylor and Francis, 1884, p. 558.
[56] S. Nemilov, G.P. Johari, Philos. Mag. 83 (2003) 3117;
S. Nemilov, G.P. Johari, Philos. Mag. 84 (2004) 845.
[57] W. Pascheto, M.G. Parthun, A. Hallbrucker, G.P. Johari, J. Non-Cryst. Solids 171 (1994) 182.
[58] C.T. Moynihan, A.J. Easteal, M.A. DeBolt, J. Tucker, J. Am. Ceram. Soc. 59 (1976) 12.
[59] G.P. Johari, Aji, J. Chem. Phys. 129 (2008) 056101.
[60] J.D. Bernal, Trans. Faraday Soc. 33 (1937) 37.
[61] A. Winter-Klein, Les causes et les effets de la trempe du verre, Rev. Opt. 16 (1937) 361.
[62] O.S. Narayanaswamy, J. Am. Ceram. Soc. 54 (1971) 491.
[63] I.M. Hodge, A.R. Berens, Macromolecules 15 (1982) 762.
[64] E. Tombari, C. Ferrari, G. Salvetti, G.P. Johari, J. Chem. Phys. 130 (2009) 124505.
[65] A. Boller, C. Schick, B. Wunderlich, Thermochim. Acta 266 (1995) 97.
[66] S.L. Simon, Thermochim. Acta 374 (2001) 55.
[67] W. Kauzmann, Chem. Rev. 43 (1948) 219.
[68] G.P. Johari, J. Chem. Phys. 113 (2000) 751.
[69] G.P. Johari, Philos. Mag. B 81 (2001) 1935.
[70] F.E. Simon, Ergebn. Exakt Naturwiss 9 (1930) 244.
[71] M. Pyda, B. Wunderlich, J. Polym. Sci. Polym. Phys. 40 (2000) 1245.
[72] D. Huang, S.L. Simon, G.B. McKenna, J. Chem. Phys. 119 (2003) 3590.
[73] G.P. Johari, J. Non-Cryst. Solids 307–310 (2002) 387.
[74] G.P. Johari, J. Chem. Phys. 116 (2002) 2043.
[75] H. Fujimori, Y. Adachi, M. Oguni, Phys. Rev. B 46 (1992) 14501.
[76] M. Hanaya, M. Nakayama, M. Oguni, J. Non-Cryst. Solids 172 (1994) 608.
[77] J.M. O'Reilly, I.M. Hodge, J. Non-Cryst. Solids 131 (1991) 451.
[78] R.W. Douglas, Br. J. Appl. Phys. 17 (1966) 435.
[79] H.S. Chen, A new aspect of glass transition, in: Proceedings of the 4th International Conference on Rapidly Solidifies Metals, Sendai, 1981, p. 495.
[80] L. Hu, Y. Yue, J. Phys. Chem. B 112 (2008) 9053, and references therein.

[81] G.P. Johari, M. Goldstein, J. Chem. Phys. 53 (1970) 2372.
[82] G.P. Johari, J. Chem. Phys. 7 (1982) 4619.
[83] G. Power, J.K. Vij, G.P. Johari, J. Chem. Phys. 124 (2006) 074509.
[84] R. Casalini, C.M. Roland, Phys. Rev. Lett. 102 (2009) 035701.
[85] I. Ichitsubo, S. Kai, H. Ogo, M. Hirao, K. Tanaka, Scripta Metall. 49 (2003) 267.
[86] T. Ichitsubo, E. Matasubara, T. Yamamoto, H.S. Chen, N. Nishiyama, J. Saida, K. Anazawa, Phys. Rev. Lett. 95 (2005) 245501.
[87] T. Ichitsubo, E. Matsubara, H.S. Chen, J. Saida, T. Yamamoto, N. Nishiyama, J. Chem. Phys. 125 (2006) 154502.